

Chapter 4

Investigation of complex anionic speciation and thermal stability of transition metal chlorides of disulfo-diisopropylammonium based acidic ionic salts and assessment of their catalytic activity in multistep one-pot synthesis of (2*E*)-ethyl 2-(arylideneamino)-6-styrylpyrimidines

4.1. Importance of styrylpyrimidine derivatives and reported methods of synthesis

Styrylpyrimidine unit is the structural motif of various medicinally important drug-like scaffolds. Some of the important styrylpyrimidine derivatives are presented in **Fig. 4.1**. 4-Styrylpyrimidines, heterocyclic analogues of *p*-aminostilbene and certain of its N-alkyl derivatives are effective inhibitors of the growth of transplanted Walker rat carcinoma. They possess an essential amino or alkylamino substituent in *o*- or *p*-position in one ring, an unsubstituted *p*-position in other ring and a *trans*-stilbene structure to mimic the activity behavior of stilbene derivatives [1]. They are evaluated as efficient inhibitors of brain choline acetyl transferase [2] and useful amyloid imaging agents for detecting B-amyloid plaques in the brain in case of Alzheimer's disease [3]. The 5-styrylpyrimidine derivatives were found to be active in micromolar concentrations in vitro against Mycobacterium tuberculosis H₃₇Rv, avium, terrae, and multidrug-resistant strain isolated from tuberculosis patients in Ural region (Russia). They were found to have a bacteriostatic effect and even higher with that of first-line antituberculosis drugs [4]. The 6-styrylpyrimidine derivatives were found to cause kidney hypertrophy in experimental animals after a single parenteral application [5]. They were also found to possess antimicrobial activity against different species of pathogenic bacteria and fungi [6]. While the 4, 6-bis(styryl) pyrimidine derivatives: the curcumin analogues were capable of exhibiting multidrug resistance reversal activity against cancer cell lines [7].

Two main routes were devised in literature for development of 4-styrylpyrimidines. Gabriel and Colman [8, 9] in 1903 synthesized the 4-styrylpyrimidine by condensing 4-methylpyrimidine with benzaldehyde by heating them with zinc chloride at 150 °C (**Scheme 4.1**). They also synthesized 2, 4-distyrylpyrimidine (**Fig. 4.2**) in a similar manner from 2, 4-dimethylpyrimidine.

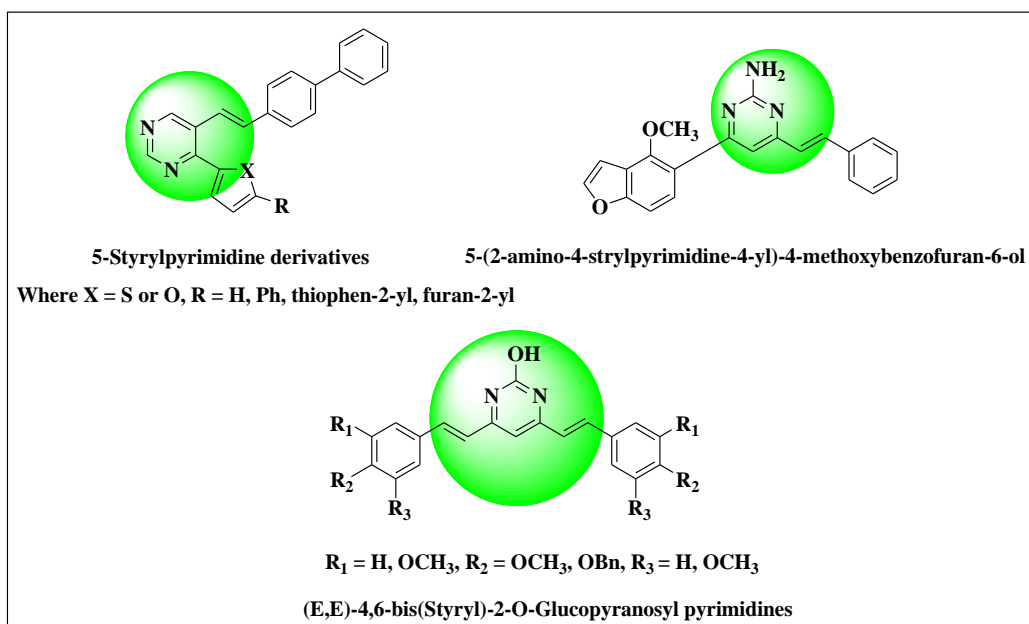
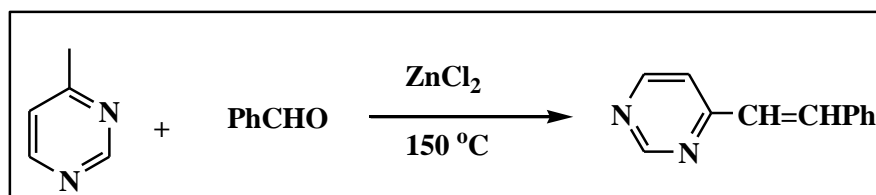


Fig. 4.1: Some important styrylpyrimidine unit containing drug-like scaffolds



Scheme 4.1: Synthesis of 4-styrylpyrimidine derivatives

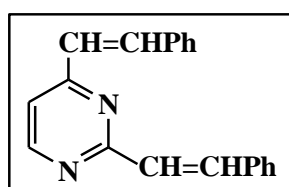


Fig. 4.2: Structure of 2, 4-distyrylpyrimidine

Bergman and Johnson [10] reported the condensation of ethyl 2-hydroxy-4-ethylpyrimidine-5-carboxylate with benzaldehyde at 180 °C without a catalyst to form the styrylpyrimidine. On the other hand, Folkers et al. [11] obtained 2-hydroxy-4-styryl-6-methyl-5, 6-dihydropyrimidine-5-carboxylic ester (**Fig. 4.3**) by the acid-catalyzed condensation of urea, ethyl acetoacetate, and cinnamaldehyde.

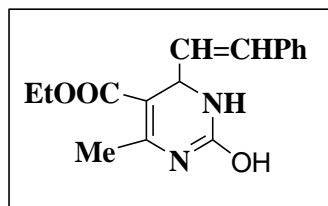
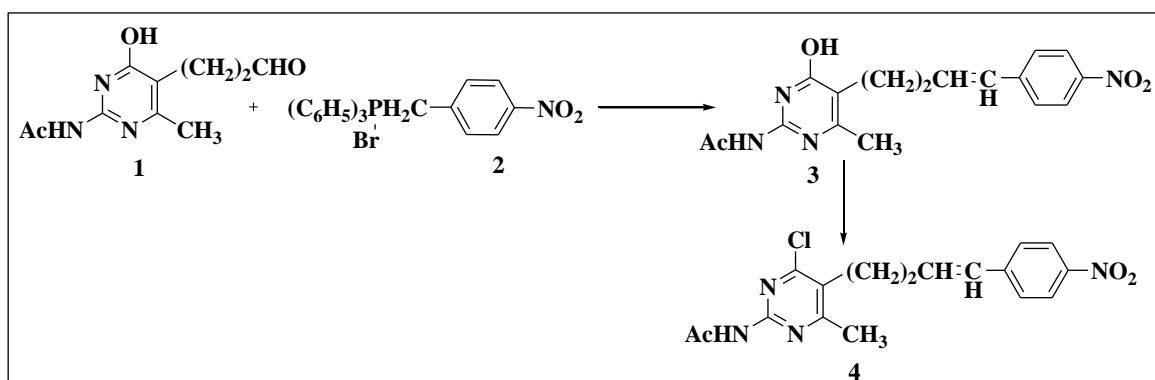


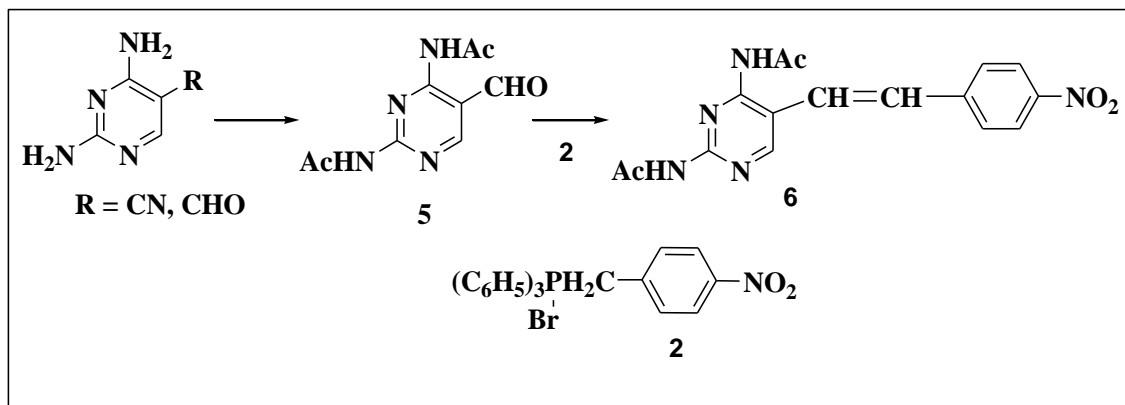
Fig.4.3: Structure of 2-hydroxy-4-styryl-6-methyl-5, 6-dihydropyrimidine-5 carboxylic ester

Loader and Timmons [12] prepared 4-trans-styryl pyrimidine through condensation of 4-methylpyrimidine with benzaldehyde in refluxing acetic anhydride within 18 h. They transformed the 4-styrylpyrimidine to benzo[f]quinazoline via photocyclodehydrogenation.

Baker et al. [13] synthesized 2-acetamido-6-methyl-5[4-(*p*-nitrophenyl)-3-butene-1-yl]-4-pyrimidinol **3** from the reaction of 2-acetamido-4-hydroxy-6-methylpyrimidine-5-propionaldehyde **1** with *p*-nitrobenzyl triphenylphosphonium bromide **2** via Wittig condensation with 69% yield. The reactions were carried out in DMF in presence of 1, 4-diazabicyclo[4.3.0] non-5-ene (DBN) as base followed by nucleophilic substitution of 4-OH to 4-Cl of compound **4** with POCl₃ (**Scheme 4.2a**). They also prepared another derivative of styryl pyrimidine **6** from the condensation reaction of 2, 4-diacetamidopyrimidine-5-carboxaldehyde **5** with *p*-nitrocinnamyl triphenylphosphonium bromide in 84% yield (**Scheme 4.2b**).



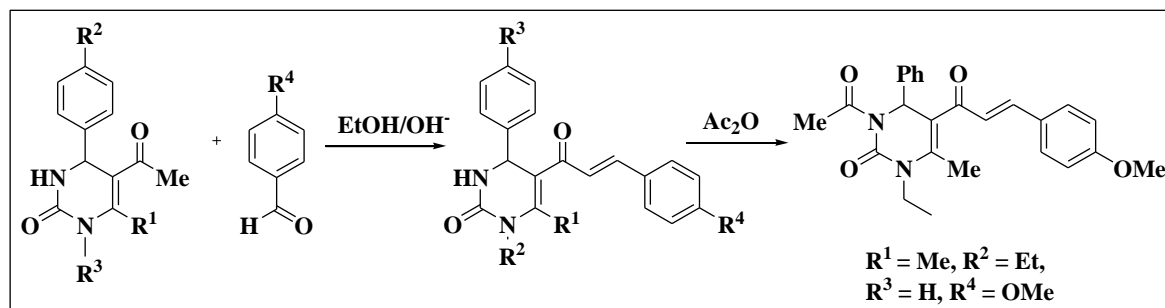
Scheme 4.2a: Preparation of styryl pyrimidine **3** and **4** reported by Baker et al.



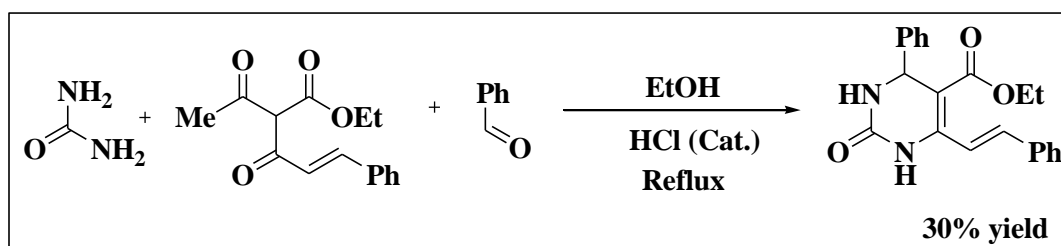
Scheme 4.2b: Synthesis of styrylpyrimidine **6** reported by Baker et al.

Gibson and Baker [14] prepared twenty two styrylpyrimidine derivatives through condensation reaction of 4-methyl amino-pyrimidine derivatives and aromatic aldehydes following the literature procedures of Loader and Timmon [12] in acetic anhydride under reflux condition, in refluxing formic acid as described by Matsukow and Suikawa [15], in acetic acid/H₂SO₄ combination as described by Saikawa and Wada [16] and also via Wittig condensation reaction of 3-chlorotriphenyl phosphonium chloride and 2, 4-diacetamido-5-pyrimidinecarboxaldehyde as described by Baker et al. [13]. They evaluated these styrylpyrimidines as inhibitors of choline acetyl transferase. The most effective inhibitors were observed with pyrimidine rings possessing two or four amino substituents.

Kolosov et al. [17] examined the Claisen-Schmidt reaction of 5-acetyl-4-aryl-3, 4-dihydropyrimidin-2(1H)-ones and obtained several number of 5-cinnamoyl- and 5-(ethoxycarbonyl)-6-styryl derivatives of 4-aryl-3, 4-dihydropyrimidin- 2(1H)-ones (**Scheme 4.3** and **Scheme 4.4**). The presence of alkyl substituent in position 1 of dihydropyrimidine ring was found to promote the Claisen-Schmidt reaction on acetyl group only; without the alkyl group both acetyl and 6-methyl groups participate in the reaction.



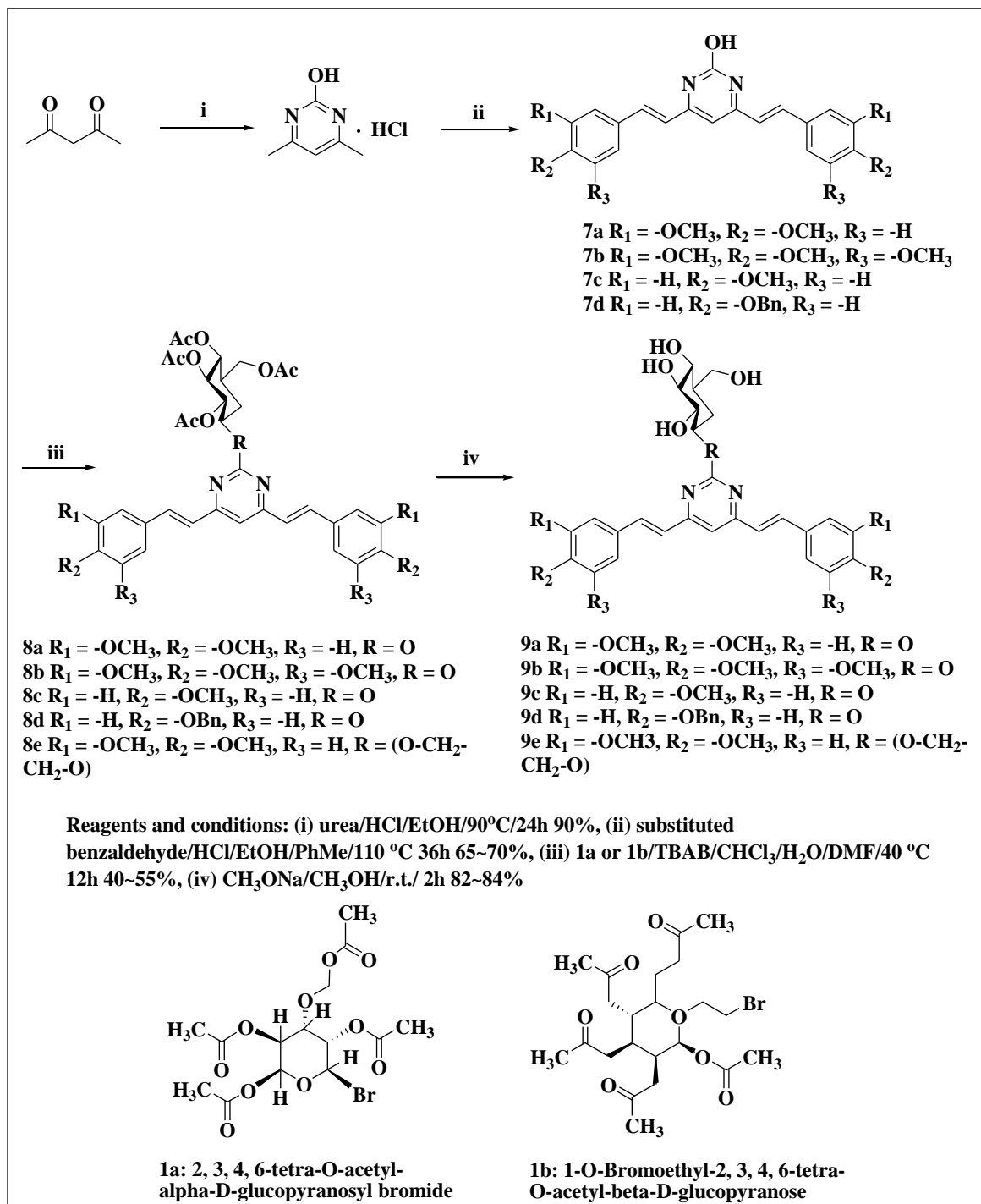
Scheme 4.3: Synthesis of 5-cinnamoyl-6-styryl derivatives of 4-aryl-3, 4-dihydropyrimidin-2(1*H*)-ones.



Scheme 4.4: Synthesis of 5-(ethoxycarbonyl)-6-styryl derivatives of 4-aryl-3, 4-dihydropyrimidin-2(1*H*)-ones

This compound was earlier prepared by Kappe and Falsone [18] from the reaction of 5-(ethoxycarbonyl)-6-methyl-4-phenyl-3, 4-dihydropyrimidin-2-one and benzaldehyde using TsOH as catalyst.

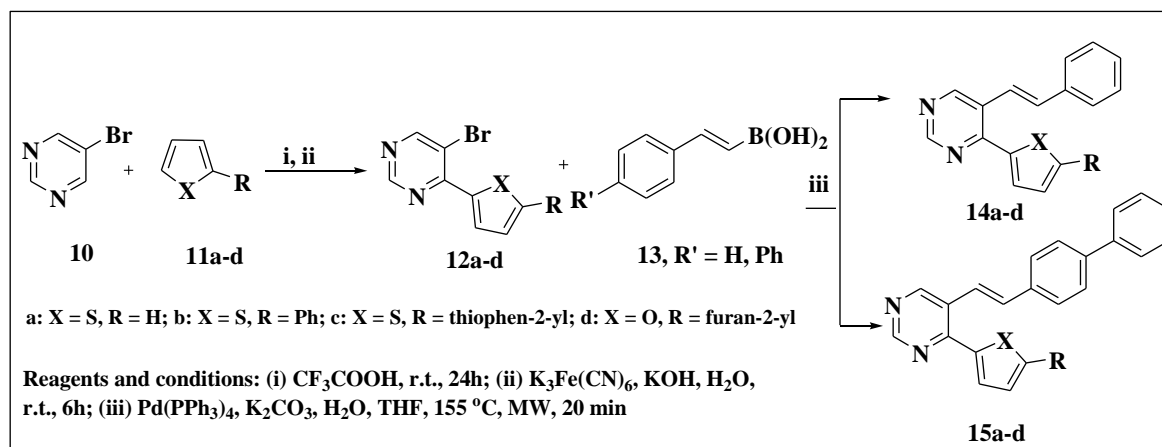
Gao et al. [19] synthesized five new styrylpyrimidines including five methoxy-or benzyloxy-substituted (*E,E*)-4, 6-bis(styryl)-2-*O*-glucopyranosyl-pyrimidines and one (*E,E*)-4, 6-bis(3, 4-dimethoxystyryl)-2-(2-*O*-glucopyranosyl)ethyloxgyl-pyrimidine in four steps with total yields of 21.5-33.9% (**Scheme 4.5**). A549 and HL60 cells were employed for anticancer activity testing which demonstrated that **9a**, **9c**, and **9e** have some inhibitory activity against the HL-60 cell line.



Scheme 4.5: Synthesis of styrylpyrimidines reported by Gao et al.

Kravchenko et al. [20] synthesized 5-styryl-4-(hetero)aryl substituted pyrimidines from commercially available 5-bromopyrimidine in combination with Suzuki cross-coupling and nucleophilic aromatic substitution of hydrogen (S_N^H) reactions (**Scheme 4.6**). The reaction intermediate 5-bromo-4-(hetero)aryl substituted pyrimidines and also the final product 5-styryl-4-(hetero)arylpyrimidines were found to be active in micromolar concentrations in vitro against *Mycobacterium tuberculosis*

H₃₇Rv, avium, terrae, and multidrug-resistant strain isolated from tuberculosis patients in Ural region (Russia).



Scheme 4.6: Synthesis of 5-styryl-4-(hetero)aryl substituted pyrimidines reported by Kravchenko et al.

The review of styrylpyrimidines reveals many potential uses of these classes of compounds for biological activities. Yet, it shows very little effort for development of efficient methodologies via multistep routes or catalytic one-pot multistep approach under environmentally benign condition.

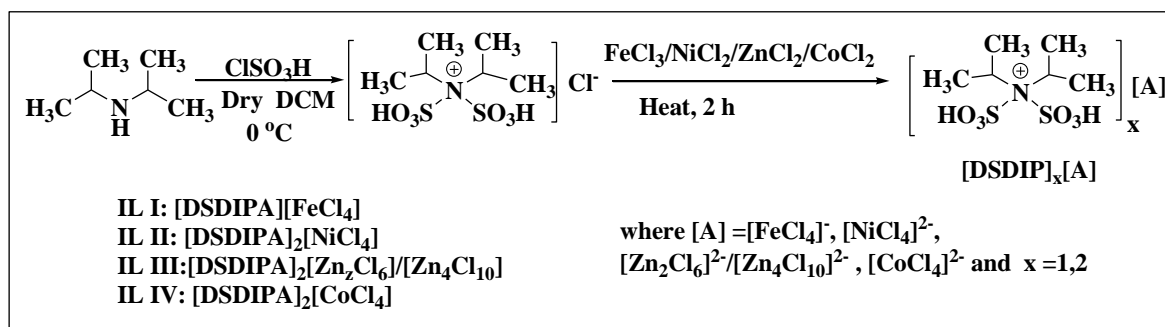
As an extension of the previous work on 2-aminopyrimidines (**Chapter 3B**), from the corresponding Biginelli DHPMs we decided to synthesize some new 6-styrylpyrimidine derivatives via condensation reactions of 2-aminopyrimidine derivatives with different aryl aldehydes.

The literature review of halometallates ionic liquids in **Chapter 1B** finds little literature on N-SO₃H functionalized imidazolium, ammonium or pyridinium chlorometallate ionic salts [21]. In continuation of the previous work of imidazolium based chlorometallates ionic salts [22], herein we aimed to synthesize another type of Brönsted-Lewis acidic ammonium based ionic salts of disulfo-diisopropyl-ammonium chlorometallates; ([DSDIP]_x[A]: where [A] = [FeCl₄]⁻, [NiCl₄]²⁻, [Zn₂Cl₆]²⁻/[Zn₄Cl₁₀]²⁻, [CoCl₄]²⁻ and x = 1, 2, (**Scheme 4.7**) and fully characterize with different analytical techniques to know their chemical composition, thermal stability, hydrophilic properties, Lewis and Brönsted acidities and also semiconductor properties. The combined study of FT-IR and UV-Vis spectroscopy provide information on the Lewis and Brönsted acidic strength of the ionic salts. The catalytic performances of these ionic

salts were explored for the multistep-one pot conversion of 2-aminopyrimidine synthesized in **Chapter 3B** to novel (2*E*)-ethyl 2-(arylideneamino)-6-styrylpyrimidine derivatives under the optimized reaction condition (**Scheme 4.8**).

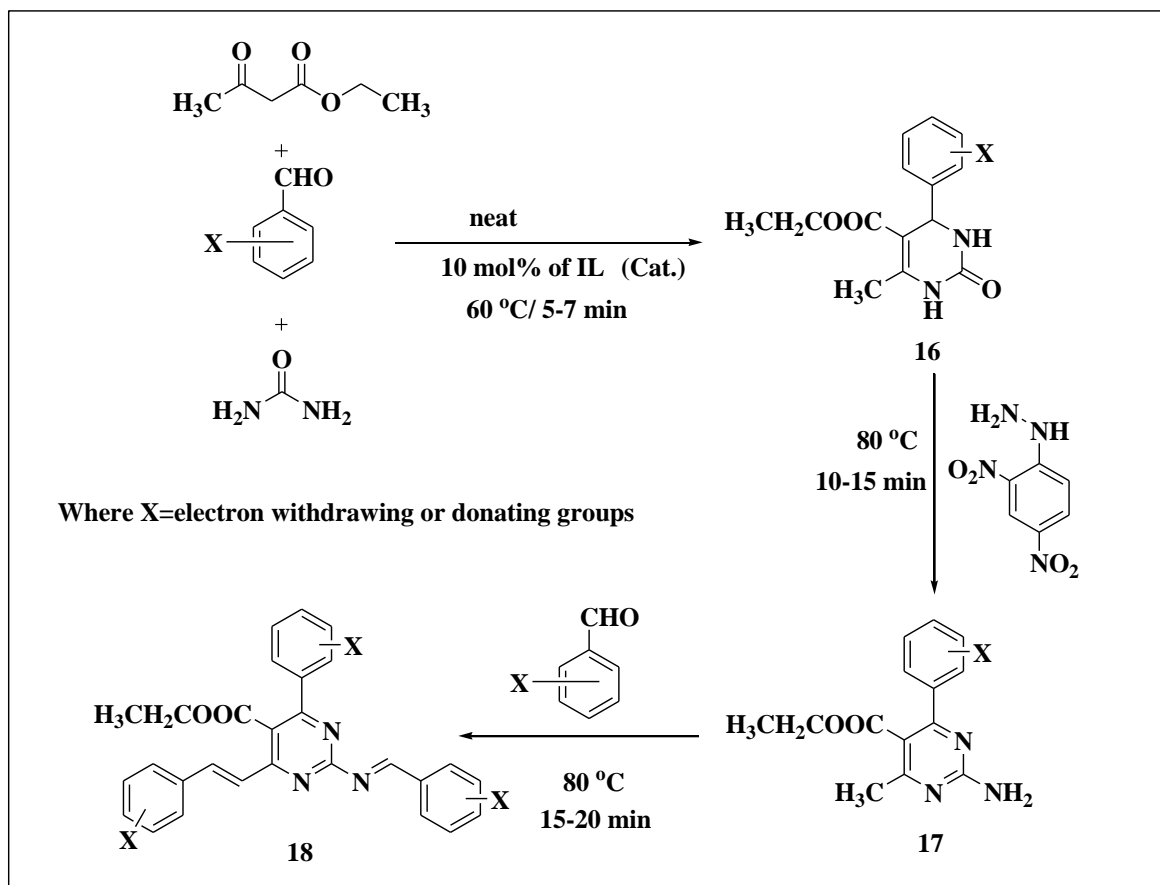
4.2. Results and discussion

Four different chlorometallates salts of disulfo-diisopropyl-ammonium ionic liquid; ([DSDIP]_x[A]: where [A]= [FeCl₄]⁻, [NiCl₄]²⁻, [Zn₂Cl₆]²⁻/[Zn₄Cl₁₀]²⁻, [CoCl₄]²⁻ with complex ionic speciation were prepared from the 1:1 reaction mixture of disulfo-diisopropyl-ammonium chloride ([DSDIP]Cl) ionic liquid with four transition metal chlorides, namely FeCl₃, ZnCl₂, NiCl₂ and CoCl₂ respectively (**Scheme 4.7**). The reactions were carried out in an inert atmosphere with continuous stirring for 2 hour at 60 °C.



Scheme 4.7: Preparation of disulfo-diisopropyl ammonium chlorometallates

All the synthesized ionic salts were investigated as reusable catalysts for one-pot three-step synthesis of (2*E*)-ethyl 2-(arylideneamino)-6-styrylpyrimidine derivatives starting from three-component Biginelli reaction involving DHPMs as the initial product (**Scheme 4.8**).



Scheme 4.8: Synthesis of (2*E*)-ethyl 2-(arylideneamino) 6-styrylpyrimidine derivatives

FT-IR and NMR studies

The four different -SO₃H functionalized diisopropyl-ammonium chlorometallate ionic salts displayed a distinctive spectral pattern in the IR region (**Fig. 4.4**). The S-O symmetric and S-O antisymmetric stretching vibrations of -SO₃H groups were confirmed from medium to strong absorptions peak obtained at 1130-1203 and 1049 cm⁻¹ respectively in addition to S-O bending vibration in the range of 613-575 cm⁻¹. The anchoring of -SO₃H group to the diisopropylamine moiety was confirmed from N-S stretching peak around 886-874 cm⁻¹. The C-N stretching characteristic peak of the diisopropylamine moiety overlapped with the S-O symmetric stretching frequency. The C-H bending characteristic of the -CH₃ group was observed at 1479-1433 cm⁻¹ while C-H bending characteristic of the gem-dimethyl group of the diisopropylamine core was observed at 1397-1377 cm⁻¹. The C-H bending characteristic of the -CH₂- group overlapped with the C-H bending region for -CH₃ group.

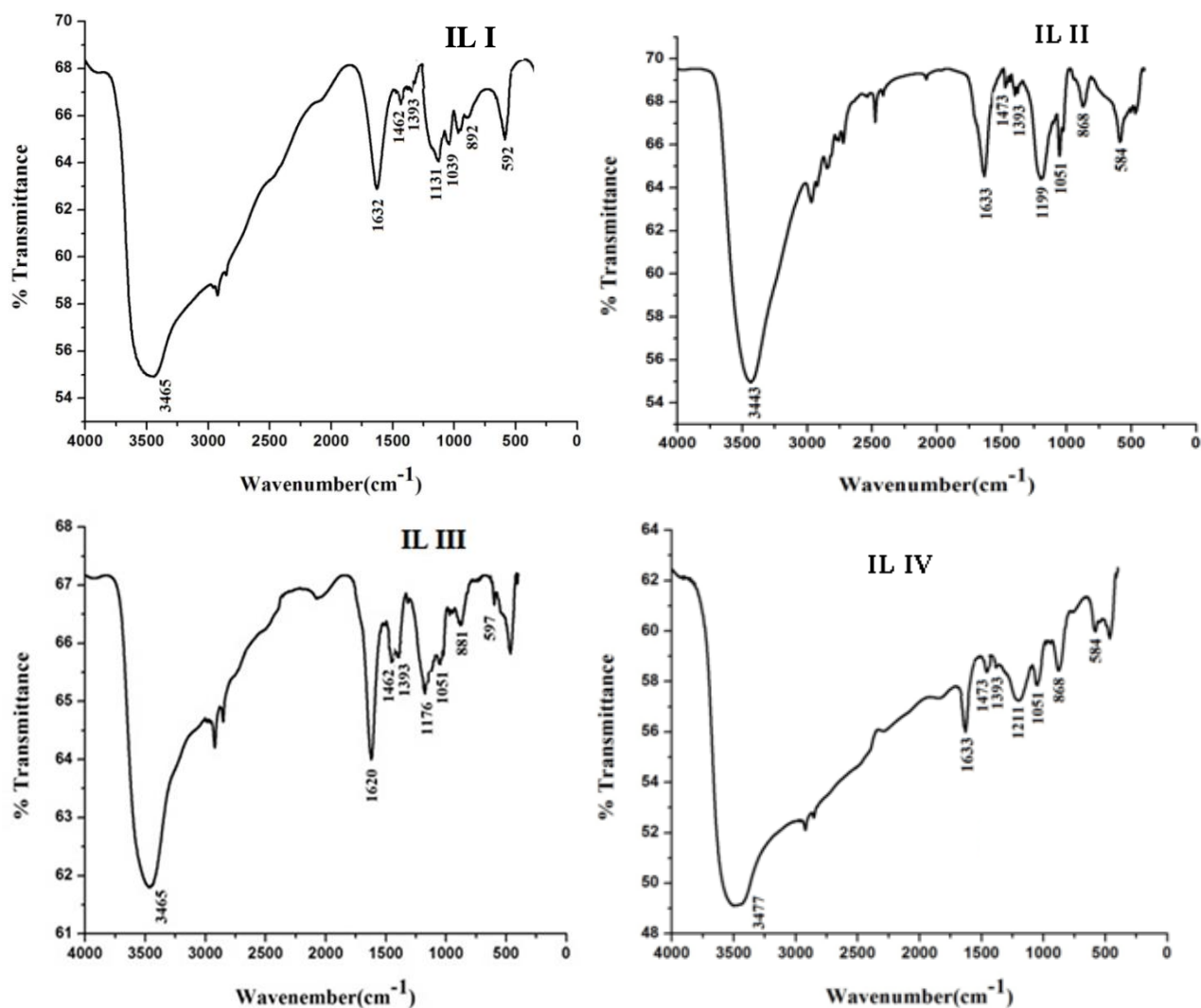


Fig. 4.4: FT-IR spectra of disulfo-diisopropyl ammonium chlorometallate

The ^1H NMR spectrum of parent ionic liquid [DSDIPA][Cl] in **Fig. 4.5(A)** identified the two acidic protons of $-\text{SO}_3\text{H}$ group as singlet at 9.95 ppm. The two equivalents $-\text{CH}$ protons of disulfo-diisopropyl ammonium cation appeared as multiplet in the range 1.94-1.90 ppm. For the 12 equivalent methyl protons, a singlet at 1.13 ppm was obtained. Similarly in ^{13}C NMR spectrum in **Fig. 4.5(B)**, two peaks at 46.0 and 19.0 ppm appeared characteristic of $-\text{CH}$ and $-\text{CH}_3$ carbons. The lower solubility of chlorometallates salts in DMSO-d_6 restricted their NMR studies.

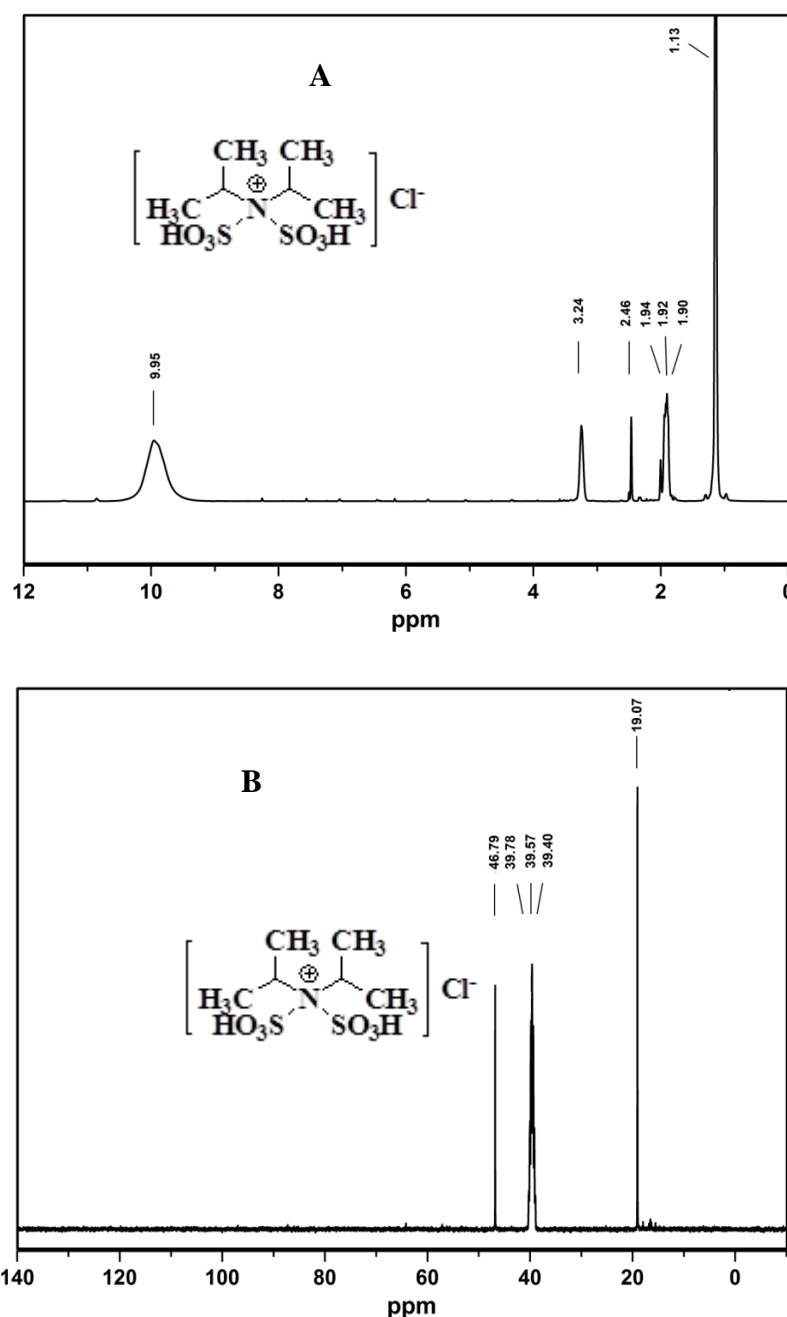


Fig. 4.5: (A) ¹H NMR and (B) ¹³C NMR spectra of [DSDPA][Cl]

Determination of anion speciation of chlorometallate salts from electronic and Raman study

The anionic speciations of the four chlorometallates ionic salts were determined from the combined electronic and Raman study.

Electronic spectral analysis

The electronic spectra of three ionic salts (**IL I**, **IL II** and **IL IV**) are represented in **Fig. 4.6** excluding **IL III** because of non-availability of required powder form of the

semi-solid sample. The sample of Fe(+2) (**IL I**) exhibited one broad absorption band near 314 nm originated from ligand to metal charge transfer transition along with d-d transition at 576 nm [23-25].

For Ni(+2) anionic complex (**IL II**), we observed ligand charge transfer transition band at 262 nm NiCl_4^{2-} [26]. It also displayed two characteristic peaks for tetrahedral NiCl_4^{2-} anionic species with comparable intensities around 700 and 773 nm [27]. The peak at 416 nm can be accounted for an equilibrium mixture of little amount of mono and dichloro nickel species with the NiCl_4^{2-} complex [26]. The analysis of electronic spectra supports the existence of most of the anionic species as tetrahedral complex of $[\text{NiCl}_4]^{2-}$.

The electronic spectra of Co(+2) anionic complex (**IL IV**) represents one triplet peak in the range of 600-700 nm with absorption maximum at 628 nm, 664 nm and 696 nm respectively. These peaks can be accounted for the ${}^4\text{T}_1(\text{P}) \rightarrow {}^4\text{A}_2(\text{F})$ transition imparting a strong gray-blue color to the ionic salt and it confirms the formation of tetrahedral $[\text{CoCl}_4]^{2-}$ complex. [27]. The formation of this species can be speculated according to equation-1.



The formation of minor amount of other cobalt-chloro complex clusters can also be expected depending on the mole fraction of CoCl_2 employed. It is supported by a literature report from Heish et al. on influence of anion speciation over electrodeposition of Co from Lewis-acidic cobalt chloride based imidazolium ionic liquids [28].

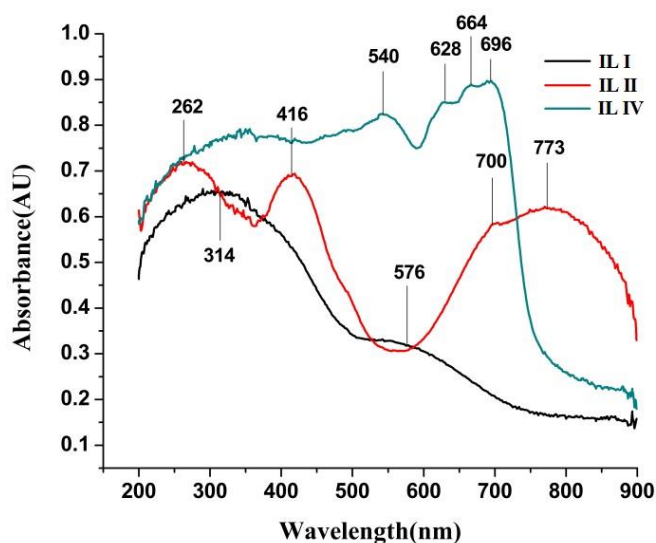


Fig. 4.6: Electronic spectra of the ionic salts

The formation of other cobalt chloride anionic speciation like CoCl_3^- , Co_2Cl_5^- and Co_3Cl_7^- clusters along with CoCl_4^{2-} might be possible from equilibrium reactions of CoCl_2 with organic chloride in presence higher mole fraction of the metal chloride employed during the preparation of this ionic salt system.

Due to weak coordination power and lower dielectric constant of tetrahedral $[\text{CoCl}_4]^{2-}$ species than CoCl_2 , it preferably absorbs UV light at a longer wavelength than other coordination-unsaturated cobalt-chloro complex clusters. In such case the characteristic absorption maximum for other complex cobalt-chloride anions like $[\text{CoCl}_3]^-$ may shift to shorter wavelength indicating the presence of a minor amount of these species along with the CoCl_4^{2-} complex. Therefore, the appearance of a weak shoulder at 545 nm for **IL IV** can be accounted for the presence of a little amount of $[\text{CoCl}_3]^-$ along with CoCl_4^{2-} complex [29].

The peak around 265 nm can be assigned for ligand to metal charge transfer transition for the tetrahedral complex of $[\text{CoCl}_4]^{2-}$ based on ligand field theory. This ionic liquid was observed as the most Lewis acidic chlorometallate salt out of the four ionic salts during Lewis acidity study via FT-IR spectra using pyridine as probe molecule.

Raman analysis

Raman study was carried out for Fe(+2), Ni(+2), and Zn(+2) metal containing chlorometallates ionic salts i.e. **IL I-III** to confirm their possible anion speciation. The Raman spectra of these ionic salts are presented in **Fig. 4.7**. The sharp peak at 350 cm^{-1} for $[\text{DSDIPA}][\text{FeCl}_4]$ confirms the anion composition as FeCl_4^- in **IL I** [30]. The Raman spectrum for **IL II** produced a sharp peak at 264 cm^{-1} which is characteristic of NiCl_4^{2-} complex [31]. For the chlorozincate system, weak-strong bands were obtained in the Raman spectrum. The strong band at 310 cm^{-1} can be ascribed to a dimeric $[\text{Zn}_2\text{Cl}_6]^{2-}$ complex with reference to a study carried out for an equimolar mixture of 1-octyl-3-methylimidazolium chloride $[\text{C}_8\text{mim}]\text{Cl}$ and ZnCl_2 [32]. Presence of a relatively weak shoulder at 282 cm^{-1} can be assigned to the T_d structure of $[\text{ZnCl}_4]^{2-}$ which may be present in lesser amount [33]. The chlorozincate system also displayed another strong band at 239 cm^{-1} and one shoulder at 360 cm^{-1} . These two peaks were found to resemble the literature data of nonlinear chlorozincate anion with molecular formulae: $[\text{Zn}_4\text{Cl}_{10}]^{2-}$

at 232 cm^{-1} and 348 cm^{-1} [34]. No absorption peaks were found corresponding to linear trinuclear $[\text{Zn}_3\text{Cl}_8]^{2-}$ complex at 288 cm^{-1} and 340 cm^{-1} in the Raman spectra of **IL III** [32,34]. In literature, the band at 232 cm^{-1} was ascribed to represent the bridging vibrations in $(\text{ZnCl}_{4/2})\text{Zn}$ with a central tetrahedral zinc for all acidic composition of the chlorozincate anion [33].

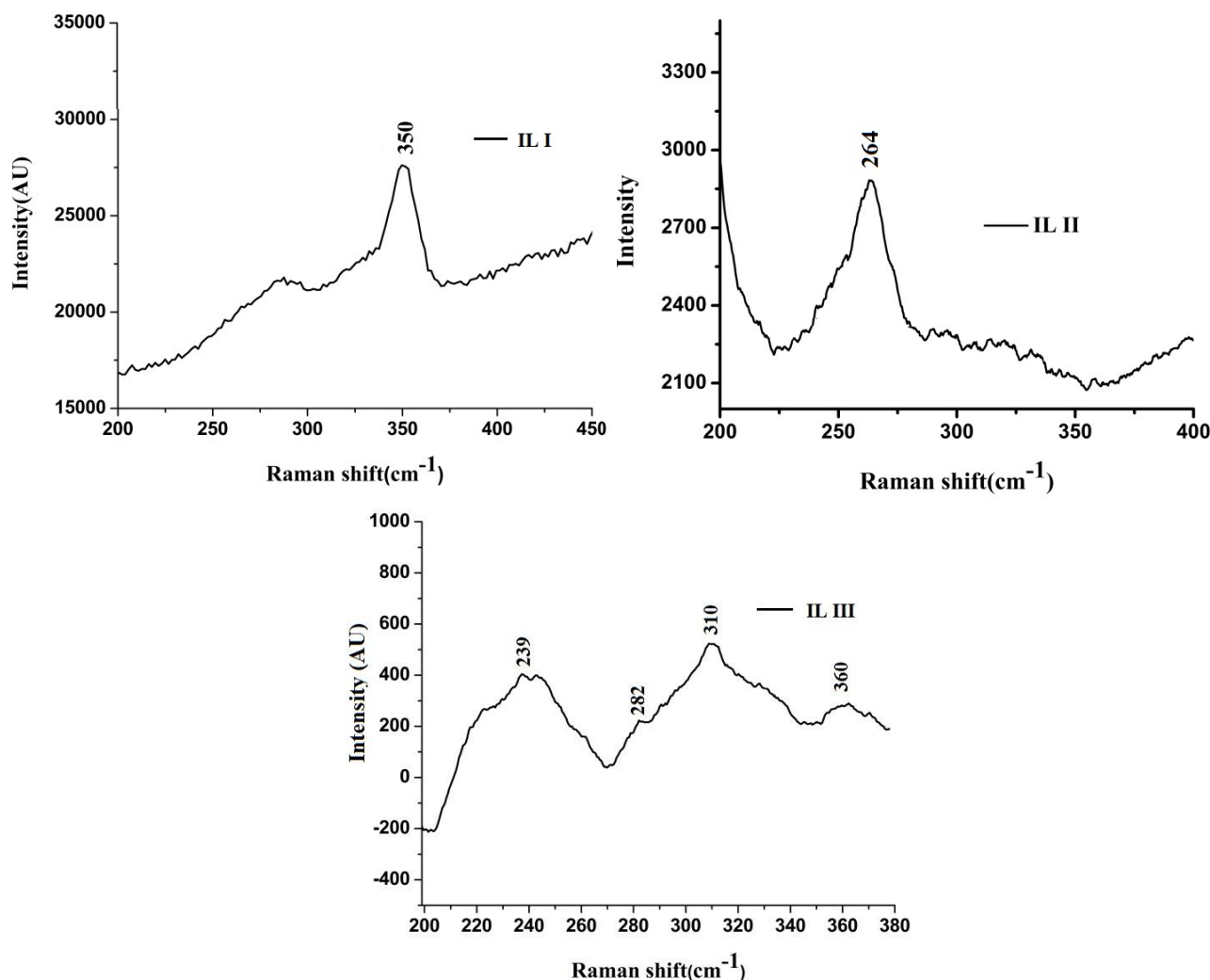


Fig. 4.7: Raman spectra of **IL I - III**

Band gap determination from Tauc plot

From the electronic spectra of four ionic salts (**Fig. 4.6**), it would be possible to estimate the semiconductor properties by calculation of optical band gap from Tauc plot (**Fig. 4.8**). The Tauc plot was generated from the Tauc equation:

$$\alpha h\nu = (h\nu - E_g)^n$$

where α is the absorption coefficient, $h\nu$ is the photon energy and E_g is the optical band gap for direct or indirect transition ($n=1/2$ or 2 respectively).

Considering the transitions to be direct and allowed type, extrapolation of the linear regime to the abscissa gave the E_g values as 2, 2.05 and 1.24 eV for **IL I**, **IL II** and **IL IV** respectively. These values are close to standard semiconductor material which signifies their importance.

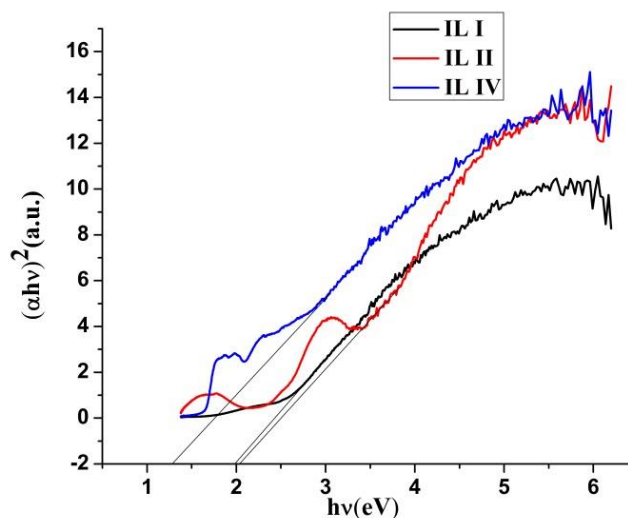


Fig. 4.8: Tauc plot for three chlorometallate ionic systems

TGA studies

The thermal stability of the chlorometallate ionic salts was assessed via TG analysis coupled with DTA and the results are shown in **Fig.4.9**. The TGA profile for the four ionic salts suggests minimum weight loss (around 2-5%) for adsorbed water below 100 °C. They witnessed variable thermal stabilities within the range of 100-130 °C. The approximate 18-20% weight loss up to 200 °C can be attributed to the loss of two $-\text{SO}_3\text{H}$ groups. It was followed by decomposition of the cationic part at once. The remaining 40-60% volatile matters of the ionic salts were completely removed around 300 °C. Weight loss above 300 °C may be attributed to the dechlorination of the complex anionic part which was further followed by oxidation of the elemental form of metals to respective oxides near around 500 °C [35].

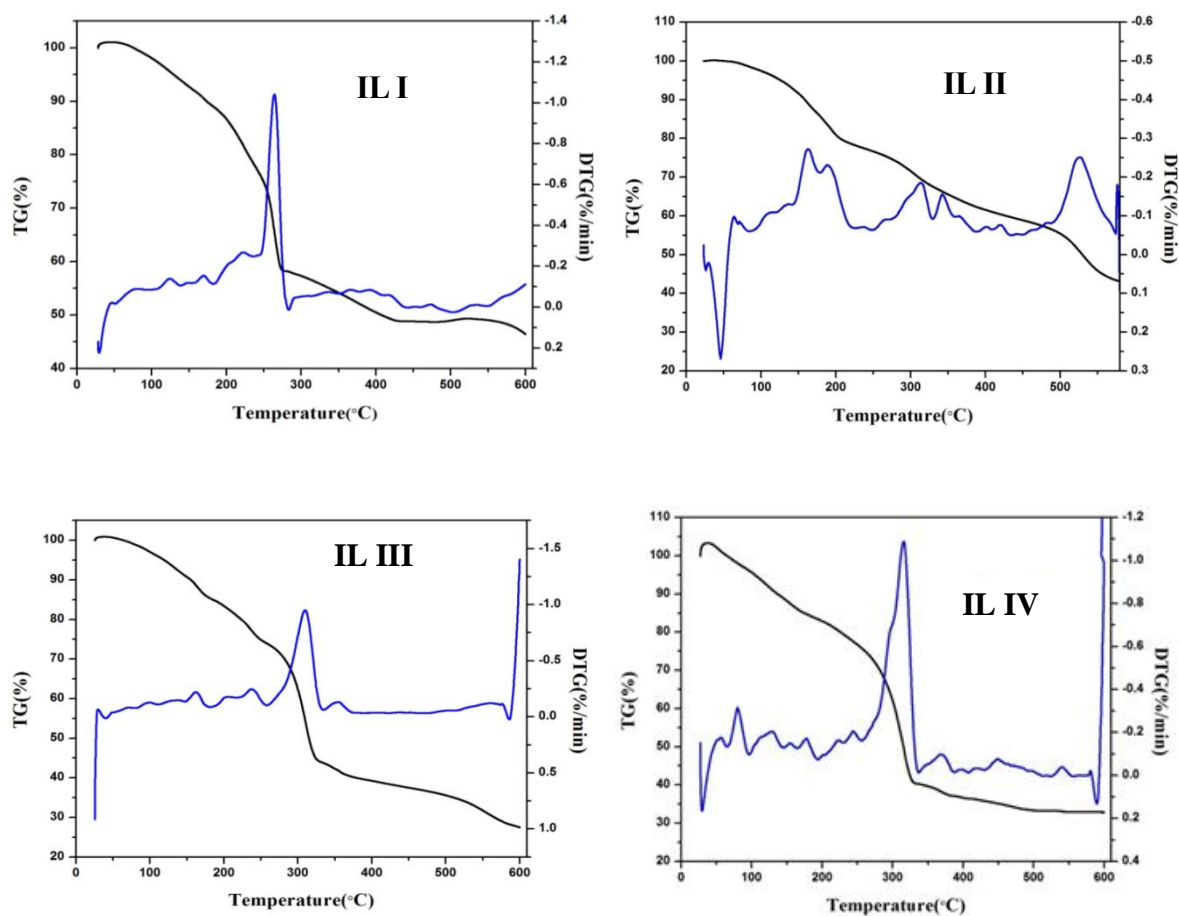


Fig. 4.9: TGA profiles for IL I- IV

Brönsted-Lewis acidity study

Determination of Lewis acidity strength of ionic salts through FT-IR spectra

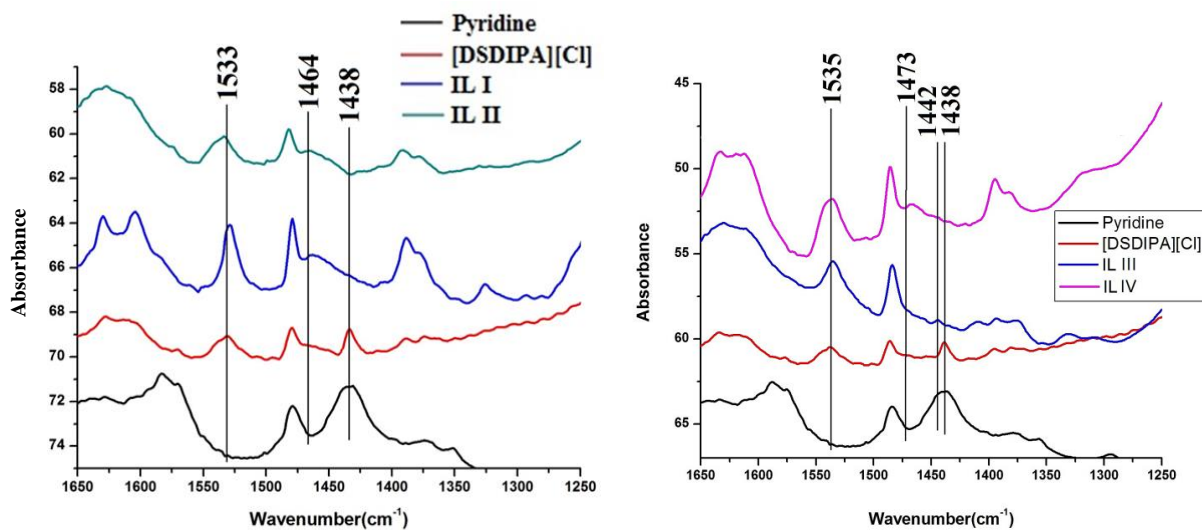


Fig. 4.10: FT-IR spectra of pyridine-IL complex

By monitoring the ring vibration modes in the range 1650-1250 cm^{-1} , pyridine can be used as a probe molecule for distinguishing Lewis/Brönsted acidic sites as well as for determination of Lewis acidic strength of the ionic salts. Neat pyridine shows a well resolved band at 1438 cm^{-1} which was unchanged in the parent ionic liquid, [DSDIPA][Cl], as there is no Lewis acidic site present. However, in the four spectra of chlorometallates, this ring vibration band of pyridine shifted towards higher wavenumber after interaction with the probe pyridine molecule (**Fig.4.10**). The characteristic wave number 1438 cm^{-1} of pyridine ring shifted to higher number such as 1463 cm^{-1} for **IL I** ([DSDIPA][FeCl₄]), 1466 cm^{-1} for **IL II** ([DSDIPA]₂[NiCl₄]), 1444 cm^{-1} for **IL III** ([DSDIPA]₂[Zn₂Cl₆]/[Zn₄Cl₁₀]) and 1474 cm^{-1} for **IL IV** [CoCl₄]²⁻. The Lewis acidic strength of these chlorometallates can be arranged in following increasing order on the basis of wave number values of pyridine ring: **IL III**<**IL I**<**IL II**<**IL IV** when mole fraction of metal chloride (χ) is =0.5. In addition to it, another band at 1533-1535 cm^{-1} arises indicating the formation of pyridinium ions resulting from the presence of Brönsted acidic sites.

Measurement of Brönsted acidity strength of ionic salts using Hammett acidity function

Quantitative assessment of the Brönsted acidity for the ionic salts was performed via UV-Vis spectroscopy from the Hammett acidity function (H^0) by following the same procedure as discussed in the previous **Chapter 1C.1** in ethanol.

Table 4.1: Brönsted acidity determination from Hammett plot

Entry	Sample name	A_{\max}	[I]%	[IH]%	H^0
1.	Indicator	0.158	100	0	-
2.	IL I	0.105	66.5	33.5	1.04
3.	IL II	0.135	85.4	14.6	1.12
4.	IL III	0.136	86.1	13.9	1.13
5.	IL IV	0.139	87.9	12.1	1.15

From the Hammett plot (**Fig. 4.11**, **Table 4.1**), the acidity order for the ionic liquid systems was estimated as: **IL IV**<**IL III**<**IL II**<**IL I**.

The overall acidity order obtained from the two different methods varied depending on the composition of anionic species and also their tendency to form secondary co-ordination shell with chloride anions in the ionic salt. The presence of small amount of CoCl_3^- anion in **IL IV** along with the $[\text{CoCl}_4]^{2-}$ can be accounted for increase in Lewis acidic sites in contrast to only one anionic speciation of Fe salt (FeCl_4^-) in **IL I**. The acidity of **IL I** was favorably controlled by the two Brønsted acidic sites of sulfonic group.

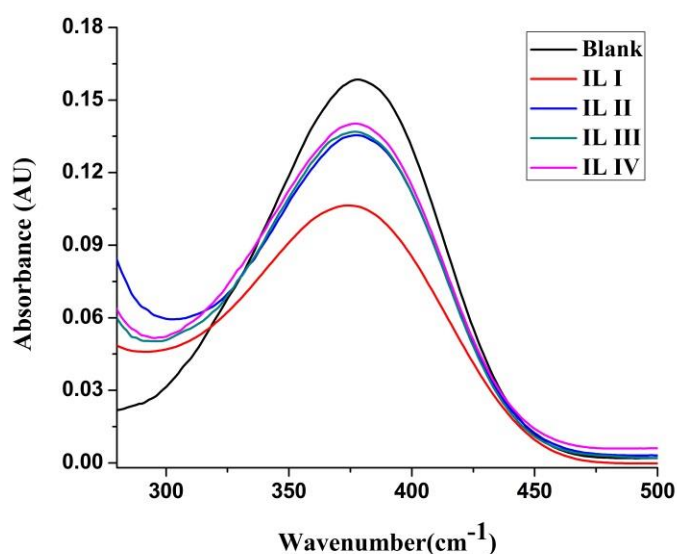


Fig. 4.11: Hammett plot of ILs

Catalytic activity evaluation

The catalytic activity of chlorometallate ionic salts were evaluated for multistep-one pot synthesis of (2*E*)-ethyl-2-(benzylideneamino)-6-styrylpyrimidine starting from three-component synthesis of Biginelli DHPMs derivatives followed by two step reactions in the same vessel according to reaction **Scheme 4.8**. For this purpose, the less hygroscopic ionic salts of Fe, Ni, and Zn metals were taken to examine their catalytic activity for the preparation of styryl pyrimidine derivatives (**18a**) under solvent-free condition at 60 °C for the 1st step and 80 °C for the next two steps in presence of 5, 10 and 15 mol% of each of the catalyst (**Table 4.2**). Out of these three ionic salts, 10 mol% of the best Brønsted acidic Fe salt **IL I** produced 75% yield of **18a** within 35 min in 3rd step from the crude mixture of 2-amino-4-benzylpyrimidine, which was prepared in 2nd step using the corresponding DHPMs (**17a**) after treatment with 2,4-dinitrophenyl hydrazine (**Table 4.2**, entry 4). Reducing the reaction temperature to 60 °C for the next

two steps using 10 mol% of **IL I** produced 65% yield of (**18a**) (**Table 4.2**, entry 6). The completions of 1st and 2nd step of reactions were monitored via thin layer chromatography technique for the specified reaction time as included in the **Table 4.2**. The optimization of catalyst amount reflected the preferential effect of Brønsted acidic site of ionic salts for catalyzing the one-pot conversion of *in situ* prepared DHPMs to styrylpyrimidine derivative (**18**). The 10 mol% of **IL I** was optimized as the best catalyst amount for synthesis of product (**18a**) (**Table 4.2**, entry 4). The optimized reaction conditions were then extended for preparation of other new styrylpyrimidinederivatives as shown in **Table 4.3** in neat condition through variation of substituted aromatic aldehydes (**Table 4.3**, entries 1-5). The plausible mechanism of acidic IL catalyzed conversion of 2-aminopyrimidine derivatives to styrylpyrimidines for the 3rd step reaction is outlined in **Scheme 4.9**.

Table 4.2: Optimization of catalyst amount for one-pot preparation of (2*E*)-ethyl-2-(benzylideneamino)-6-styrylpyrimidine (**18a**)

Entry	Catalyst	Amount of catalyst (mol %)	Time ^a			% yield ^{b,c} (18a)
			Step I	Step II	Step III	
1	IL I	15	3	10	10	75
2	IL II	15	5	18	15	69
3	IL III	15	10	20	18	64
4	IL I	10	5	10	15	75
5	IL I	5	10	25	20	64
6	IL I	10	5	15	35	65

^aFor entry number 1-5, reactions were carried out at 60 °C for the 1st step and 80 °C for the next two steps;

^bAll the three steps for entry 6 was conducted at 60 °C; ^cIsolated yield

Table 4.3: Substrate scope study with 10 mol % of **IL I** for substituted aromatic aldehydes

Entry	Aldehyde	Time (min)			% Yield ^{a, b} (18a-e)
		Step I	Step II	Step III	
1	C ₆ H ₅ CHO	5	10	15	75 (18a)
2	4-CH ₃ C ₆ H ₄ CHO	7	15	20	72 (18b)

3	2,4-(Cl) ₂ C ₆ H ₃ CHO	5	10	15	70 (18c)
4	4-ClC ₆ H ₄ CHO	5	15	18	68 (18d)
5	4-NO ₂ C ₆ H ₄ CHO	5	10	15	73 (18e)

^aIsolated yield; ^bAll reactions were performed using the optimized reaction temperature.

Catalyst recyclability study

Reusability study for **IL I** was carried out using 10 mol% of the catalyst in 3 mmol scale reaction for the synthesis of **18a** (Fig. 4.12). The activity of the IL slightly decreased with increased cycle of reactions. After completion of the reaction, DCM was added to the reaction mixture to separate it from the catalyst. The catalyst was further washed with hot ethanol and dried in vacuum oven to activate it for next cycle of reaction. The decreased activity of the IL can be ascribed to the loss of metal chlorides during washing with hot ethanol which ultimately leads to destroyal of the catalytic moiety in course of the reactivation process.

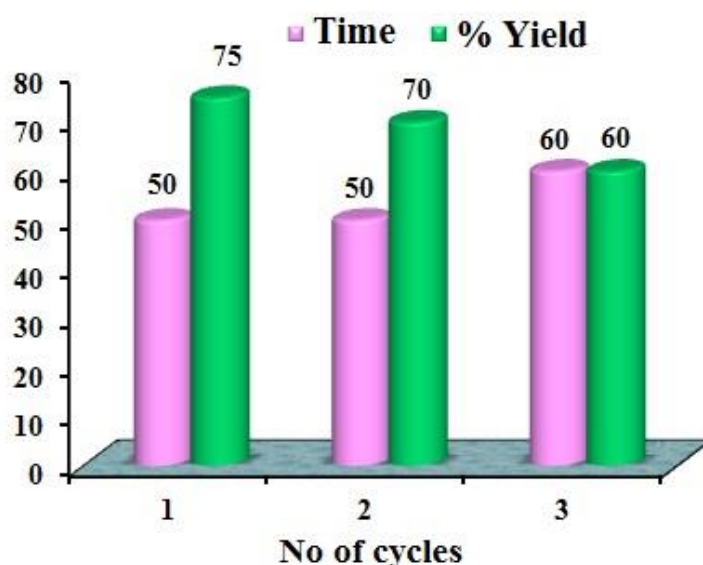
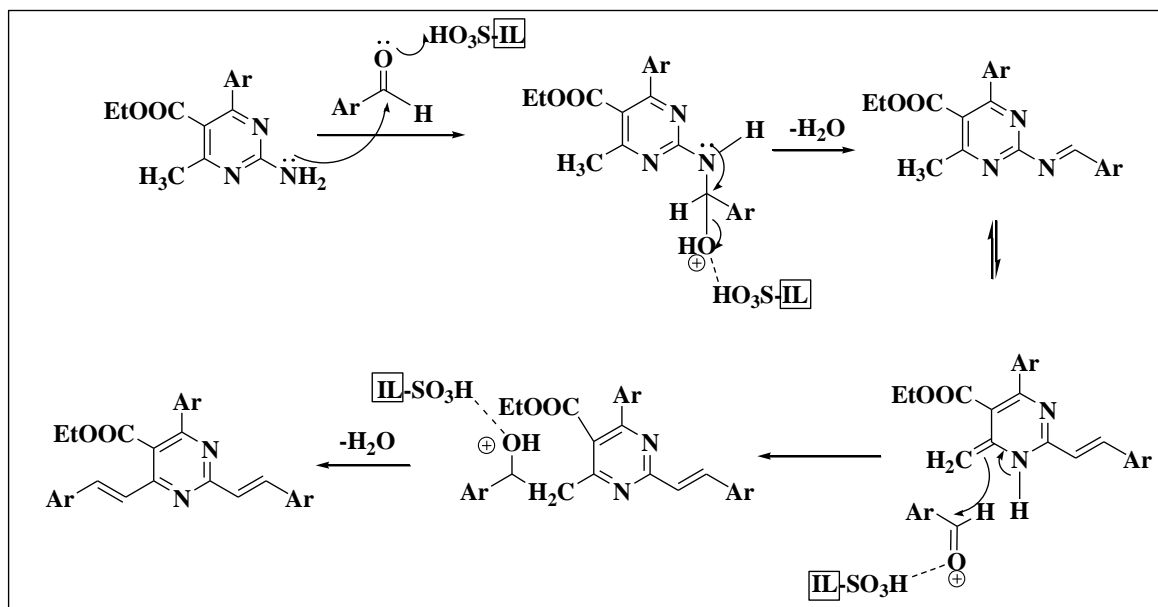


Fig. 4.12: Recyclability profile of **IL I** for preparation of **18a**



Scheme 4.9: Plausible mechanism for synthesis of styrylpyrimidine derivatives

The used catalyst after 3rd run was analyzed via FT-IR study (**Fig. 4.13**) to check the intactness of the chlorometallate salt. The chlorometallate salt **IL I** retains its characteristic vibration pattern up to 3rd cycle with slight changes of peak positions.

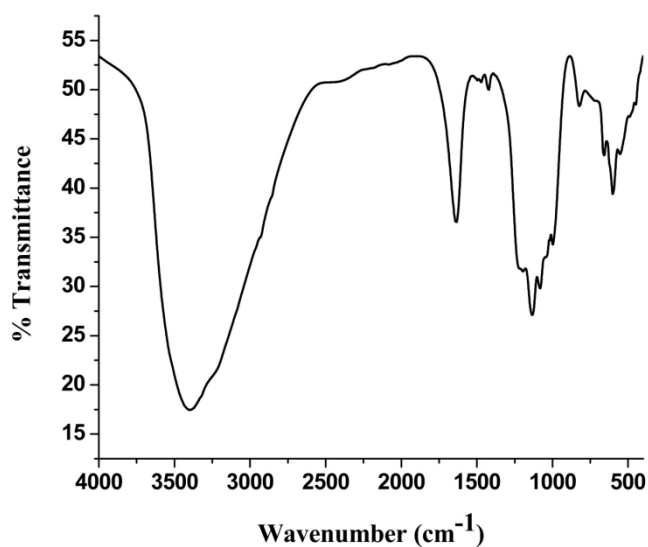


Fig. 4.13: FT-IR analysis of the used catalyst (**IL I**)

4.3. Conclusion

Four new chlorometallate salts of disulfodiisopropylammonium chloride (DSDIPA)[Cl] ionic liquid were successfully synthesized and characterized with various analytical techniques. The anionic speciation of the chlorometallate salts were examined using the combined indicative studies of FT-IR, Raman and electronic spectroscopy. In conjunction with literature support, the co-ordination sphere of metal anionic species have been proposed and expressed accordingly based on the analysis data in these chlorometallate salts. These chlorometallate ionic liquids displayed variable thermal stabilities within the range of 100-130 °C with loss of minimum amount of adsorbed water (~2-5%) below 100 °C. From the acidity study, it was found that the overall Brönsted and Lewis acidity order for these salts depend on the anionic speciation and also their tendency to form secondary co-ordination shell in presence of excess amount of chloride anion present in the ionic liquid salt. Out of these two acidic sites, the Brönsted acidic site has major role for catalyzing the three-step one pot synthesis of styrylpyrimidine derivatives without isolating the two intermediates formed in the 1st and 2nd steps under solvent-free thermal method.

4.4. Experimental section

All chemicals were purchased from reputed chemical suppliers. The chlorometallate ionic liquids were fully characterized via FT-IR, ¹H and ¹³C NMR, Diffused Reflectance spectroscopy (DRS), Raman and TGA-DTG techniques. The DR spectra were recorded on a UV 2450, Shimadzu spectrophotometer. The qualitative assessment of the Lewis-Brönsted acidity of the chlorometallates was done on a FT-IR spectrophotometer using dry pyridine as the molecular probe. The quantitative Brönsted acidity of the ionic salts was determined using a UV-Vis spectrophotometer.

Synthetic procedure for synthesis of ([DSDIPA]_x[A]) ionic salts ; where [A]= [FeCl₄], [NiCl₄]²⁻, [Zn₂Cl₆]²⁻/[Zn₄Cl₁₀]²⁻, [CoCl₄]²⁻ and x =1,2

The three chlorometallate ionic salts were prepared by a two-step reaction (**Scheme 4.7**). The first step involved through dropwise addition of chlorosulfonic acid (20 mmol) to a stirred solution of diisopropylamine (10 mmol) in dry CH₂Cl₂ (30 mL) at 0 °C within a period of 5 min under nitrogen atmosphere in a 100 mL round bottom flask. Then the mixture was stirred for one hour to complete the synthesis of disulfo-

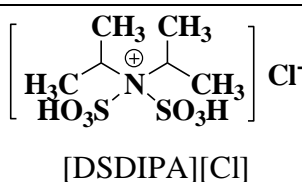
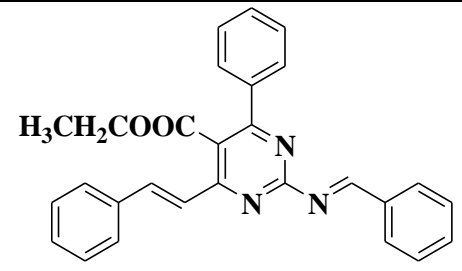
diisopropyl ammonium chloride [DSDIPA][Cl]. The viscous ionic liquid layer was washed three times with fresh CH_2Cl_2 (3×10 mL) by decantation of dichloromethane solution. The residue was dried under vacuum which produced 98% pale yellow viscous oil of [DSDIPA][Cl]. The 2nd step was performed by mixing equimolar amount of respective metal chlorides with the [DSDIPA][Cl] at 60 °C for 2 hour with continuous stirring. The crude molten product was cooled to room temperature and washed with dry DCM to eliminate any residual parent IL. The solid-semi solid ionic salts were dried in vacuum to yield the desired chlorometallateionic systems with brown (**IL I**=87% yield), yellowish green (**IL II**=85% yield), light brown (**IL III**=90% yield), bluish grey (**IL IV**=84% yield) color respectively.

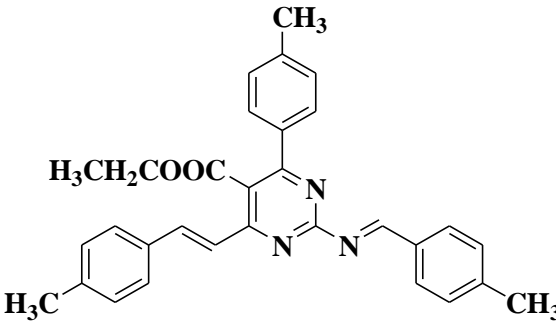
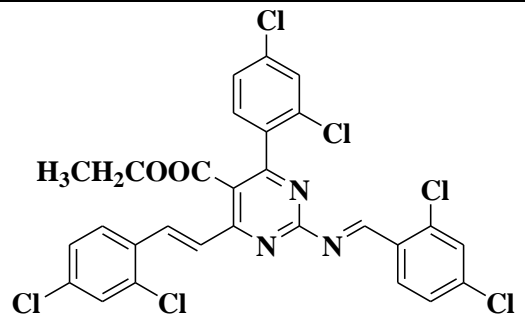
Synthesis of (2E)-ethyl 2-(benzylideneamino) 6-styrylpyrimidine derivatives (Scheme 4.8):

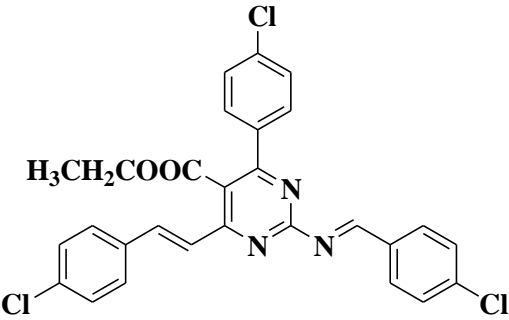
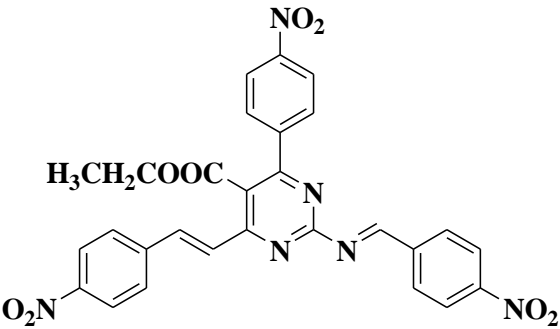
A three component mixture of ethyl acetoacetate (1 mmol), aromatic aldehyde (1 mmol) and urea (1.5 mmol) was treated in a two necked 50 mL round bottom flask at 60 °C for 5-15 min using 10 mol% of **IL I**. The formation of 3, 4-dihydropyrimidin-2-(*IH*)-one was confirmed by thin layer chromatography (TLC) in presence of EtOAc and hexane (1:3) as developing solvent. After completion of the 1st step, 1 mmol of 2, 4-dinitro-phenylhydrazine was added to the crude mixture along with few drops of dichloromethane and then heated at 80 °C for 10-15 min. The progress of 2nd step was also tracked with TLC technique using 1:5 ratios of EtOAc and hexane as solvent system. Finally, the addition of 2 mmol of aromatic aldehydes was done to the crude product of 2-amino pyrimidine derivative at once after completion of the 2nd step as monitored by TLC method. The 3rd step was conducted in the same temperature within the specified reaction time as given in the **Table 4.3**. The work-up step involved with addition of 6 mL of CH_2Cl_2 to crude reaction mixture for separation of unreacted DHPMs and chlorometallate catalyst as solid residue through filtration of dichloromethane solution of the crude mixture of product and remaining 2, 4-dinitrophenyl hydrazine substrate. Then the catalyst was again recovered as solid residue on filter paper by filtration of hot solution of DHPMs in ethanol. Cooling of the saturated solution of styrylpyrimidines and 2,4-dinitrophenyl hydrazine in dichloromethane at 0 °C precipitated out 2, 4-dinitro-phenyl hydrazine as red solid. Evaporation of the DCM solution yielded the crude styrylpyrimidine derivatives as solid

residue which was further recrystallized from saturated methanol solution to get analytically pure solid (*2E*)-ethyl 2-(benzylideneamino) 6-styrylpyrimidines with 68-75% (**3a-e**) yields. The three-step sequential reaction required almost 30-45 min time to produce satisfactory yield of product.

4.5. Spectral data of ILs and styrylpyrimidine derivatives

Product	Spectral data
 <p>[DSDIPA][Cl]</p>	<p>Pale yellow liquid; FT-IR(KBr): 3427, 1637, 1470, 1197, 1055, 1024, 876, 851, 591, 579, 462 cm⁻¹; ¹H NMR (400 MHz, DMSO-d₆): δ 9.95 (s, 2H), 2.0-1.9 (m, 2H), 1.12 (d, <i>J</i> = 4 Hz, 12H); ¹³C NMR (100 MHz, DMSO-d₆): δ 46, 19.</p>
 <p>(Table 4.3, entry 1)</p>	<p>(2E)-Ethyl-2-(benzylideneamino)-4-phenyl-6-styrylpyrimidine-5-carboxylate 18a; Yellow solid; M.P.(°C): 217-228; FT-IR(KBr): 3285, 3108, 3089, 2926, 1699, 1725, 1615, 1585, 1516, 1486, 1446, 1367, 1327, 1314, 1274, 1220, 1132, 1086, 1069, 1053, 1020, 953, 825, 758, 690, 613, 532, 506, 420 cm⁻¹; ¹H NMR (400 MHz, CDCl₃): δ 1.21-1.17 (m, 3H), 4.14-4.09 (m, 2H), 5.47 (s, 1H), 5.90 (s, 1H), 7.09 (d, <i>J</i> = 16 Hz, 1H), 7.34-7.30 (m, 8H), 7.49-7.45 (d, <i>J</i> = 16 Hz, 3H), 7.77 (s, 1H), 7.86 (s, 1H), 8.12-8.03 (m, 2H); ¹³C NMR (100 MHz, CDCl₃): δ 165.2, 152.9, 148.0, 147.9, 143.3, 142.9, 135.6, 134.1, 133.1, 131.0, 130.0, 129.3, 129.0, 128.8, 128.1, 127.5, 126.7, 123.5, 120.0, 116.8, 103.1, 60.4, 14.1; CHN analysis(%): C₂₈H₂₃N₃O₂, cal C 77.58 H 5.35 N 9.69; found C 77.50, H 5.46 N 9.67.</p>

 <p>(Table 4.3, entry 2)</p>	<p>(2E)-Ethyl-2-(4-methylbenzylideneamino)-4(4-methylstyryl)-6-(4-methylphenyl)pyrimidine-5-carboxylate 18b; Light orange solid; M.P.(°C): 214.2-216.3; FT-IR(KBr): 3285, 3224, 3090, 2923, 1703, 1688, 1615, 1504, 1466, 1419, 1327, 1313, 1290, 1266, 1226, 1172, 1135, 1096, 1080, 969, 930, 896, 817, 724, 714, 671, 614, 520 cm⁻¹; ¹H NMR (400 MHz, DMSO-d₆): δ 8.81 (s, 1H), 8.62 (s, 1H), 8.33 (d, <i>J</i> = 8.0 Hz, 1H), 8.03 (d, <i>J</i> = 12.0 Hz, 1H), 7.87 (d, <i>J</i> = 16 Hz, 1H), 7.65(d, <i>J</i> = 8 Hz, 2H), 7.37(d, <i>J</i> = 8.0 Hz, 2H), 7.27 (d, <i>J</i> = 8.0 Hz, 2H), 7.20 (d, <i>J</i> = 8.0 Hz, 2H), 7.14-7.08 (m, 3H), 5.18(s, 1H), 4.04 (m, 2H), 2.32-2.28 (m, 5H), 2.22 (s, 2H), 1.15 (t, <i>J</i> = 8 Hz, 3H); ¹³C NMR (100 MHz, DMSO-d₆): δ 166.8, 153.1, 150.1, 145.0, 142.0, 141.1, 139.3, 137.4, 135.2, 133.8, 131.6, 130.3, 130.1, 129.5, 126.7, 123.6, 119.1, 117.3, 102.3, 60.3, 21.7, 21.5, 21.2, 14.6 CHN analysis(%): C₃₁H₂₉N₃O₂, cal C 78.29 H 6.15 N 8.84; found C 78.26, H 6.21 N 8.83.</p>
 <p>(Table 4.3, entry 3)</p>	<p>(2E)-Ethyl-2-(2,4-dichlorobenzylideneamino)-4(2,4-dichlorostyryl)-6-(2,4-dichlorophenyl)pyrimidine-5-carboxylate 18c; Yellow solid; M.P.(°C): 251.3-253.2; FT-IR(KBr): 3360, 3280, 3096, 2965, 1701, 1614, 1587, 1535, 1516, 1499, 1471, 1420, 1326, 1309, 1285, 1264, 1222, 1136, 1092, 1058, 1047, 925, 827, 769, 740, 604, 522 cm⁻¹; ¹H NMR (400 MHz, DMSO-d₆): δ 7.71(s, 1H), 7.68-7.67 (m, 4H), 7.52-7.46 (m, 4H), 7.36(d, <i>J</i> = 8.0 Hz, 1H), 7.28(d,</p>

	<p>$J = 8.0$ Hz, 1H), 5.55 (s, 1H), 3.84 (q, $J = 8.0$ Hz, 2H), 0.96 (t, $J = 8.0$ Hz, 3H); ^{13}C NMR (100 MHz, DMSO-d_6): δ 158.7, 144.7, 139.1, 135.9, 134.6, 130.9, 130.2, 128.5, 123.4, 117.6, 59.7, 14.4.; CHN analysis(%): $\text{C}_{28}\text{H}_{17}\text{Cl}_6\text{N}_3\text{O}_2$, cal C 52.53 H 2.68 N 6.56; found C 52.54, H 2.72 N 6.55.</p>
 <p>(Table 4.3, entry 4)</p>	<p>(2E)-Ethyl-2-(4-Chlorobenzylideneamino)-4(4-chlorostyryl)-6-(4-chlorophenyl)pyrimidine-5-carboxylate 18d; Yellow solid; M.P.($^{\circ}\text{C}$): 264.6-268.4; FT-IR(KBr): 3285, 3090, 2920, 2852, 1613, 1584, 1515, 1489, 1422, 1402, 1327, 1223, 1137, 1082, 825, 614, 509 cm^{-1}; ^1H NMR (400 MHz, DMSO-d_6): δ 8.36-8.33 (dd, $J = 12$ Hz, 4 Hz, 2H), 8.08 (d, $J = 8.0$ Hz, 2H), 7.79(d, $J = 8.0$ Hz, 4H), 7.72 (br, 1H), 7.53 (d, $J = 8.0$ Hz, 4H), 7.36 (d, $J = 8.0$ Hz, 1H), 5.10 (s, 1H) 3.94 (q, $J = 8.0$ Hz, 2H), 1.04 (t, $J = 8.0$ Hz, 3H); ^{13}C NMR (100 MHz, DMSO-d_6): δ 164.8, 154.8, 148.5, 144.9, 137.7, 133.2, 130.3, 129.6, 123.5, 117.4, 53.9, 15.7.; CHN analysis(%): $\text{C}_{28}\text{H}_{20}\text{Cl}_3\text{N}_3\text{O}_2$, cal C 62.64 H 3.76 N 7.83; found C 62.63, H 3.77 N 7.82.</p>
 <p>(Table 4.3, entry 5)</p>	<p>(2E)-Ethyl-2-(4-nitrobenzylideneamino)-4(4-nitrostyryl)-6-(4-nitrophenyl)pyrimidine-5-carboxylate 18e; Orange solid; M.P.($^{\circ}\text{C}$): 242.2-245; FT-IR(KBr): 3434, 3303, 2925, 2851, 1705, 1595, 1570, 1510, 1492, 1344, 1261, 1147, 1109, 909, 847, 751, 690, 501 cm^{-1}; ^1H NMR (400 MHz, DMSO-d_6): δ 8.39 (dd, $J = 8.0$ Hz, 4 Hz, 2H), 8.29 (d, $J = 8.0$ Hz, 2H), 8.19 (d, $J = 12.0$ Hz, 2H),</p>

	8.13 (d, $J = 8.0$ Hz, 2H), 7.99 (d, $J = 12$ Hz, 4H), 7.85 (broad singlet, 1H), 7.47 (d, $J = 8$ Hz, 1H), 5.22 (s, 1H), 3.95 (q, $J = 8.0$ Hz, 2H), 1.01 (t, $J = 8.0$ Hz, 3H); ^{13}C NMR (100 MHz, DMSO- d_6): δ 165.6, 152.5, 148.5, 147.1, 144.7, 140.6, 138.4, 130.4, 128.7, 128.2, 124.7, 124.4, 123.4, 117.6, 54.2, 14.6.; CHN analysis(%): $\text{C}_{28}\text{H}_{20}\text{N}_6\text{O}_8$, cal C 59.16 H 3.55 N 14.78; found C 59.16, H 3.58 N 14.76.
--	--

References

1. Ross, W. C. J. 224. Some derivatives of 4-styrylpyrimidine. *Journal of the Chemical Society (Resumed)*, 1128-1135, 1948.
2. Gibson, R. E. and Baker, B. R. Enzyme inhibitors. Inhibition of brain choline acetyltransferase by derivatives of 4-styrylpyrimidine. *Journal of medicinal chemistry*, 17(12):1290-1293, 1974.
3. Labib, A. A. Synthesis, radioiodination and biodistribution evaluation of 5-(2-amino-4-styryl pyrimidine-4-yl)-4-methoxybenzofuran-6-ol. *Asia Oceania Journal of Nuclear Medicine and Biology*, 1(1):32-38, 2013.
4. Kravchenko, M. A., Verbitskiy, E. V., Medvinskiy, I. D., Rusinov, G. L., and Charushin, V. N. Synthesis and antituberculosis activity of novel 5-styryl-4-(hetero) aryl-pyrimidines via combination of the Pd-catalyzed Suzuki cross-coupling and S N H reactions. *Bioorganic & Medicinal Chemistry Letters*, 24(14):3118-3120, 2014.
5. Ingerowski, R. M., Haux, F., and Bruchhausen, F. V. Decreased prostaglandin synthetase activity during kidney regeneration after folic acid or 2, 4, 5-triamino-6-styrylpyrimidine application. *Naunyn-Schmiedeberg's Archives of Pharmacology*, 298(2):157-162, 1977.
6. Dhankar, R. P., Rahatgaonkar, A. M., Chorghade, M. S., and Tiwari, A. Spectral and in vitro antimicrobial properties of 2-oxo-4-phenyl-6-styryl-1, 2, 3, 4-tetrahydro-pyrimidine-5-carboxylic acid transition metal complexes.

- Spectrochimica Acta Part A: Molecular and Biomolecular Spectroscopy*, 93:348-353, 2012.
7. Gao, L., Liu, Q., Ren, S., Wan, S., Jiang, T., Wong, I. L., Chow, L. M., and Wang, S. Synthesis of a novel series of (E, E)-4, 6-bis (styryl)-2-O-glucopyranosyl-pyrimidines and their potent multidrug resistance (MDR) reversal activity against cancer cells. *Journal of Carbohydrate Chemistry*, 31(8):620-633, 2012.
 8. Gabriel, S. and Colman, J. Zur Kenntniss des pyrimidins und methylierter pyrimidine. *European Journal of Inorganic Chemistry*, 36(3):3379-3385, 1903.
 9. Kondo, H. and Yanai, M. Ueber die Kondensation von 2, 4, 6-Trimethylpyrimidin und Benzaldehyd. (I. Mitteilung), *Yakugaku Zasshi*, 57(7):747-751, 1937.
 10. Bergmann, W. and Johnson, T.B. Die synthese des 5-acetyl-uracils (untersuchungen über pyrimidine, CXXXVII. Mitteil.). *European Journal of Inorganic Chemistry*, 66(10):1492-1496, 1933.
 11. Folkers, K., Harwood, H. J., and Johnson, T. B. Researches on pyrimidines. Cxxx. Synthesis of 2-keto-1, 2, 3, 4-tetrahydropyrimidines. *Journal of the American Chemical Society*, 54(9):3751-3758, 1932.
 12. Loader, C. E. and Timmons, C. J. Studies in photochemistry. Part III. The photocyclisation of 4-styrylpyrimidine to benzo [f] quinazoline. *Journal of the Chemical Society C: Organic*, 1343-1344, 1967.
 13. Baker, B. R. and Meyer Jr, R. B. Irreversible enzyme inhibitors. CLI. Active-site-directed irreversible inhibitors of dihydrofolic reductase derived from 5-(p-aminophenylbutyl)-2, 4-diaminopyrimidines with a terminal phenylene sulfonyl fluoride. *Journal of Medicinal Chemistry*, 12(2):224-227, 1969.
 14. Baker, B. R. and Meyer Jr, R. B. Irreversible enzyme inhibitors. CLIV. Some factors in cell wall transport of active-site-directed irreversible inhibitors of dihydrofolic reductase derived from 5-substituted 2, 4-diaminopyrimidines. *Journal of medicinal chemistry*, 12(4):668-671, 1969.
 15. Matsukow, T. M. and Suikawa, K. Reactions of 2-aminopyrimidines with aromatic aldehydes. I, *Yakugaku Zasshi*, 72(7):909-912, 1952.
 16. Saikowa, I. and Wada, T. Japanese PATENT 20,978(1965) Chem. Abstr., 64, 2105, 1966.

17. Kolosov, M. A., Orlov, V. D., Vashchenko, V. V., Shishkina, S. V., and Shishkin, O. V. 5-Cinnamoyl-and 5-(Ethoxycarbonyl)-6-styryl derivatives of 4-Aryl-3, 4-dihydropyrimidin-2 (1H)-ones. *Collection of Czechoslovak Chemical Communications*, 72(9):1219-1228, 2007.
18. Falsone, F. S. and Kappe, C. O., The Biginelli dihydropyrimidone synthesis using polyphosphate ester as a mild and efficient cyclocondensation/dehydration reagent. *Arkivoc*, 2(ii):122-134, 2001.
19. Gao, L., Liu, Q., Ren, S., Wan, S., Jiang, T., Wong, I. L., Chow, L. M., and Wang, S. Synthesis of a novel series of (E, E)-4, 6-bis (styryl)-2-O-glucopyranosyl-pyrimidines and their potent multidrug resistance (MDR) reversal activity against cancer cells. *Journal of Carbohydrate Chemistry*, 31(8):620-633, 2012.
20. Kravchenko, M. A., Verbitskiy, E. V., Medvinskiy, I. D., Rusinov, G. L., and Charushin, V.N. Synthesis and antituberculosis activity of novel 5-styryl-4-(hetero) aryl-pyrimidines via combination of the Pd-catalyzed Suzuki cross-coupling and S N H reactions. *Bioorganic & Medicinal Chemistry Letters*, 24(14):3118-3120, 2014.
21. Estager, J., Holbrey, J. D., and Swadźba-Kwaśny, M. Halometallate ionic liquids–revisited. *Chemical Society Reviews*, 43(3):847-886, 2014.
22. Gogoi, P., Dutta, A. K., Sarma, P., and Borah, R. Development of Brønsted–Lewis acidic solid catalytic system of 3-methyl-1-sulfonic acid imidazolium transition metal chlorides for the preparation of bis (indolyl) methanes. *Applied Catalysis A: General*, 492:133-139, 2015.
23. Mineralurgii, F. P. Extraction of zinc (II), iron (III) and iron (II) with binary mixtures containing tributyl phosphate and di (2-ethylhexyl) phosphoric acid or Cyanex 302. *Physicochemical Problems of Mineral Processing*, 36:217-224, 2002.
24. Bäcker, T., Breunig, O., Valldor, M., Merz, K., Vasylyeva, V., and Mudring, A. V. In-situ crystal growth and properties of the magnetic ionic liquid [C2mim][FeCl4]. *Crystal Growth & Design*, 11(6):2564-2571, 2011.
25. Kogelnig, D., Stojanovic, A., vd Kammer, F., Terzieff, P., Galanski, M., Jirsa, F., Krachler, R., Hofmann, T., and Keppler, B. K. Tetrachloroferrate containing

- ionic liquids: Magnetic-and aggregation behavior. *Inorganic Chemistry Communications*, 13(12):1485-1488, 2010.
26. Khokhryakov, A. A., Mikhaleva, M. V., and Paivin, A. S. Electronic absorption spectra of nickel dichloride and nickel oxide solutions in the 2CsCl-NaCl and KCl-NaCl melts. *Russian Journal of Inorganic Chemistry*, 51(8):1311-1314, 2006.
27. Kettle, S. F. A. *Physical Inorganic Chemistry: A Coordination Chemistry Approach*, Oxford University Press, New York, 1998.
28. Hsieh, Y. T., Lai, M. C., Huang, H. L., and Sun, I. W. Speciation of cobalt-chloride-based ionic liquids and electrodeposition of Co wires. *Electrochimica Acta*, 117:217-223, 2014.
29. Rao, A. P. and Dubey, S. P. Synergistic effects in ion exchange in mixed solvents-chloride media. *Analytical Chemistry*, 44(4):686-691, 1972.
30. Wang, L., Lu, B., Zhu, A., Sun, H., and Shen, Q. Development of Fe (III)-containing ether-functionalized imidazolium ionic liquids for aryl Grignard cross-coupling of alkyl halides. *Science Bulletin*, 30(58):3624-3629, 2013.
31. Yan, C., Wang, L., Gao, H., Sun, H., and Shen, Q. An efficient and recyclable iron (III)-containing imidazolium salt catalyst for cross-coupling of aryl Grignard reagents with alkyl halides. *Chinese Science Bulletin*, 57(16):1953-1958, 2012.
32. Estager, J., Nockemann, P., Seddon, K. R., Swadźba-Kwaśny, M., and Tyrrell, S. Validation of speciation techniques: a study of chlorozincate (II) ionic liquids. *Inorganic Chemistry*, 50(11):5258-5271, 2011.
33. Quicksall, C. O. and Spiro, T. G. Raman spectra of tetrahalozincates and the structure of aqueous ZnCl_4^{2-} . *Inorganic Chemistry*, 5(12):2232-2233, 1966.
34. Yannopoulos, S. N., Kalampounias, A. G., Chrissanthopoulos, A., and Papatheodorou, G. N. Temperature induced changes on the structure and the dynamics of the “tetrahedral” glasses and melts of ZnCl_2 and ZnBr_2 . *The Journal of Chemical Physics*, 118(7):3197-3214, 2003.
35. Haines P. *Thermal Methods of Analysis Principles, Applications and Problems*, 1st Edition, Springer Science and Business Media, 1995.